

Article

Not peer-reviewed version

Effect of Graphene Nanoplatelets as Lubricant Additive on Fuel Consumption During Vehicle Emission Tests

[Eduardo Tomanik](#)*, [Wania Christinelli](#), Pamela Sierra Garcia, Scott Rajala, Jesuel Crepaldi, [Davi Franzosi](#), [Roberto Martins Souza](#), [Fernando Fusco Rovai](#)

Posted Date: 9 January 2025

doi: 10.20944/preprints202412.0909.v2

Keywords: Graphene; Friction; Fuel Economy; viscosity



Preprints.org is a free multidisciplinary platform providing preprint service that is dedicated to making early versions of research outputs permanently available and citable. Preprints posted at Preprints.org appear in Web of Science, Crossref, Google Scholar, Scilit, Europe PMC.

Copyright: This open access article is published under a Creative Commons CC BY 4.0 license, which permit the free download, distribution, and reuse, provided that the author and preprint are cited in any reuse.

Effect of Graphene Nanoplatelets as Lubricant Additive on Fuel Consumption During Vehicle Emission Tests

Eduardo Tomanik ^{1,2*}, Wania Christinelli ¹, Pamela Sierra Garcia ¹, Scott Rajala ³, Jesuel Crepaldi ⁴, Davi Franzosi ², Roberto Martins Souza ² and Fernando Fusco Rovai ^{5,6}

¹ Gerdau Graphene Brazil

² Surface Phenomena Laboratory, Polytechnic School of the University of Sao Paulo

³ Idemitsu Lubricants America Corp.

⁴ Idemitsu Lube South America Ltda

⁵ VW do Brasil – Way to Zero Center

⁶ Department of Mechanical Engineering, Centro Universitário FEI

* Correspondence: eduardo.tomanik@gmail.com

Abstract: Lubricant friction modifier additives are used on lower-viscosity engine oils to mitigate boundary friction. This work presents the development of a graphene-based material as oil friction modifier additive, from formulation to actual vehicle tests. The Graphene material was initially characterized using scanning electron microscopy (SEM) and Raman spectroscopy, which revealed the predominance of graphene nanoplatelets (GNP) with an average of 9 layers. After functionalization, two GNP additive variants were initially mixed with a fully formulated SAE 0W-20 engine oil and tribologically evaluated using reciprocating sliding tests at 40 and 120 °C and Hertzian pressure up to 1.2 GPa when both variants presented friction reduction. Then, the GNP additive variant with better performance was evaluated in a vehicle emission test using a fully formulated 5W-20 SAE oil as a reference. The addition of 0.1% of GNP reduced fuel consumption by 2.6% in Urban conditions and 0.8% in Highway ones. The urban test cycle was the FTP75 and higher benefits of the GNP additive occurred especially on test start, when the engine and oil are still cold and on test portions where the vehicle speed is lower.

Keywords: graphene; friction; fuel economy; viscosity

1. Introduction

The search for reducing fuel consumption and CO₂ emission has led to continuous efforts for reducing the mechanical losses caused by friction. For combustion engines, lower viscosity oils are being introduced to reduce engine-dominant hydrodynamic friction losses but with the risk of increasing boundary friction [1,2]. To protect engine parts against potential damage related to metal-to-metal contact, due to the increasing trend in reducing oil viscosity, some lubricant formulation strategies are applied. These initiatives include introducing the right type of friction modifier, choosing high viscosity index base oils and selecting efficient viscosity index improvers based on olefin copolymers to minimize shear thinning, as demonstrated in previous works [3–6].

On [5] different types of FM additives (MoDTC, three variants based on ester polymer and an Amine based one) were tested in TE-77 rotational and floating liner reciprocating testers. The tested MoDTC additive provided the highest reductions in friction force and friction losses. Combining those efforts with engine adaptations to operate in the presence of ultra-low viscosity oils, results of fuel economy at homologation test cycles may reach values up to 5.5% depending on the baseline oil of a given engine, as shown in [7,8].

More recently, nanoparticles are being investigated as lubricant additives. Spikes [9] has mentioned five potential advantages of using nanoparticles as lubricant additives: (1) insolubility in nonpolar base oils; (2) low reactivity with other additives in the lubricant; (3) high possibility of film formation on many different types of surfaces; (4) more durability; and (5) high nonvolatility to withstand high temperatures. Different elements have been investigated as nanoparticles, including metals, ceramics, chalcogenides, MXenes and carbon-based materials [9–16]. Lubricants with nanoparticles are also called “Nanolubricants”, with the nanoparticles acting as anti-wear or friction modifier. However, these solutions usually require the use of dispersants and surfactants to functionalize the nanoparticles as oil additive. [11,13,14]. Carbon-based nano materials include Carbon dots, Carbon Nanotubes (CNT), Graphene, Graphene Oxide and others [13,14]. Graphene-based materials, due to unique properties such as low shear resistance, high stiffness, and thermal conductivity, are attractive materials for tribological applications, including improvement on the properties of lubricants. [13,14]. The exact mechanism that improves the tribological performance is still being investigated and probably more than one occurs on actual applications. Figure 1 summarizes the main potential tribological mechanisms of nanoparticles. Graphene and other nanosheets may also work as viscous modifier, see discussion on [13].

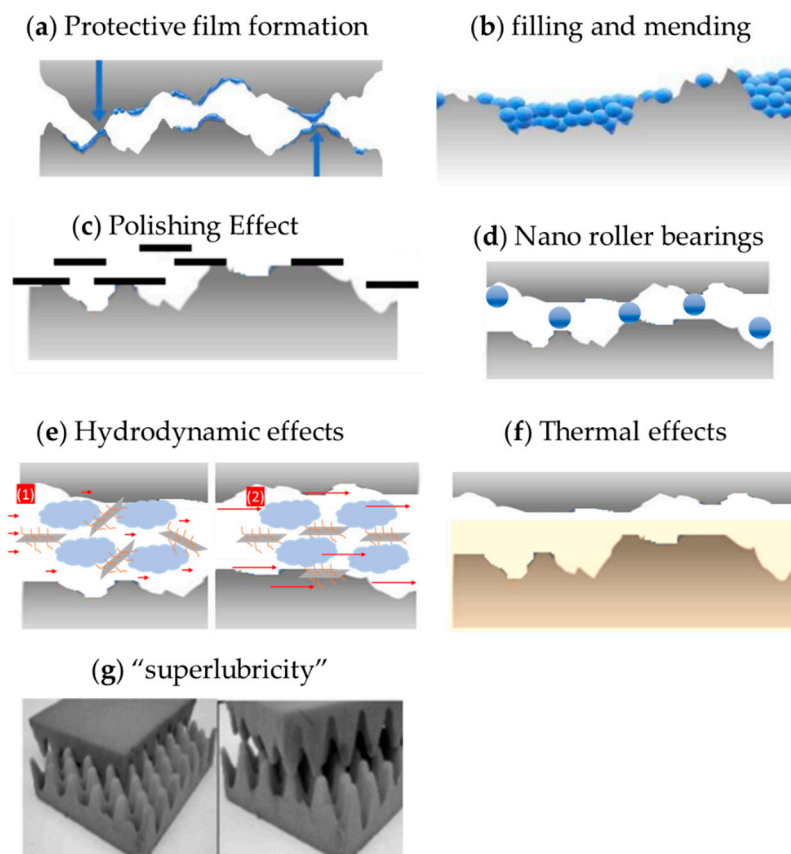


Figure 1. Graphene’s tribological mechanisms. (a) Typical FM tribofilm (b) Surface filling and mending (c) Polishing effect (d) nano roller bearings (e) Hydrodynamics at (1) low shear rate, (2) high shear rate. (f) Thermal effects (g) Superlubricity, incommensurable contact. Reproduced from [9].

Synergic or antagonistic mechanisms with other oil additives as well as with the materials in contact may occur [17]. In summary, despite all the research already done, there are several knowledge gaps about the use of nanoparticles as lubricant additives. Especially for engine oils, it appears mandatory to test fully formulated oils and test on actual applications. Following the steps of formulation and initial characterization of a given engine oil, the evaluation of the tribological behavior usually starts with laboratory tests [5,6]. Despite the importance that these initial tests have, it is frequently difficult to evaluate how much a difference in coefficient of friction in laboratory represents in terms of the overall performance of real engines, for example in terms of fuel

consumption. Factors that contribute to these difficulties include: i) the relatively large fuel consumption dispersion on actual vehicle tests ii) the impact on the efficiency of other energy losses (e.g. thermal) [8] and iii) the diversity of tribological systems inside an engine, each one with specific tribological conditions including lubrication regimes that can vary from boundary to hydrodynamic [2]. The use of laboratory data as inputs to numerical simulations of an engine, or of a specific system within, may help to bridge the gap between laboratory and engine tribological results [1,2].

This work aims to cover all the main steps mentioned in the paragraphs above. Two variations of graphene-based additives of engine oil were developed and characterized. Laboratory lubricated reciprocating sliding tests were then conducted with these oils, to evaluate the friction reduction potential. Finally, the investigation was completed by vehicle tests to compare fuel consumption when oils with or without the additive were used. Graphene-based materials, due to unique properties such as low shear resistance, high stiffness, and thermal conductivity, are attractive materials for tribological applications, including improvement on the properties of lubricants. [9,10].

2. Materials and Methods

2.1. Graphene Characterization

Graphene samples, after deposition as a powder over a conductive carbon adhesive tape, were characterised by scanning electron microscopy (SEM) using a Hitachi SU5000 model. Raman spectroscopy was used to characterize the structure of the samples using an Oxford Instruments (Ulm, Germany) Witec Alpha 300 RA equipment with a 532 nm laser. A typical Raman spectrum of graphene has three main bands that describe the crystalline quality of the material and stacking characteristics, such as the number of coupled interlayers. The D band, located at 1350 cm^{-1} , is activated by the disorder generated at 1580 cm^{-1} , caused by stretching the C-C covalent bonds common in all carbon systems with sp^2 hybridization. The 2D band, located at approximately 2700 cm^{-1} , is the over-tone of the D band, with two transverse optical phonons.

Raman spectra were the inputs of an improved version of the protocol described in [18] to quantify crystalline defects and the number of graphene-coupled interlayers (see Table 1 and Figures 2 and 3). The GNP has on average 9 layers and a lateral size of 71.1 nm. The diagram (b) in the figure 2 was proposed by Silva et al [18] and analyzes the crystalline structure of graphene, considering the crystallite size and the distance between point defects as a function of the G band width, and the ratio of the areas of the D and G bands multiplied by the laser energy used for the measurement to the fourth power. In the diagram, the values of larger crystallite size and greater distance between point defects (which would define fewer defective samples) are in the lower left corner of the diagram. As the defects in the structure increase, the position in the diagram shifts upwards and to the right. Thus, it is possible to observe that the graphene used in this work has a preserved crystalline structure, with low defect density. Under higher magnification SEM, it is possible to notice that its sheets are aggregated in a spherical manner (Figure 4).

Table 1. GNP characterization.

Characteristic	Unit	Mean	Q90
Number of layers - $\langle N \rangle_{2D}$ (nm)	-	9	11
Surface density of point defects - n_D	10^{10} cm^{-2}	2.8	4.3
Lateral size - L_a	nm	71.1	99.4
D to G peak intensity ratio (I_D/I_G)		0.28	0.44
Percentile of volume-based particle size distribution		9.6 (D_{50})	19.3 (D_{90})

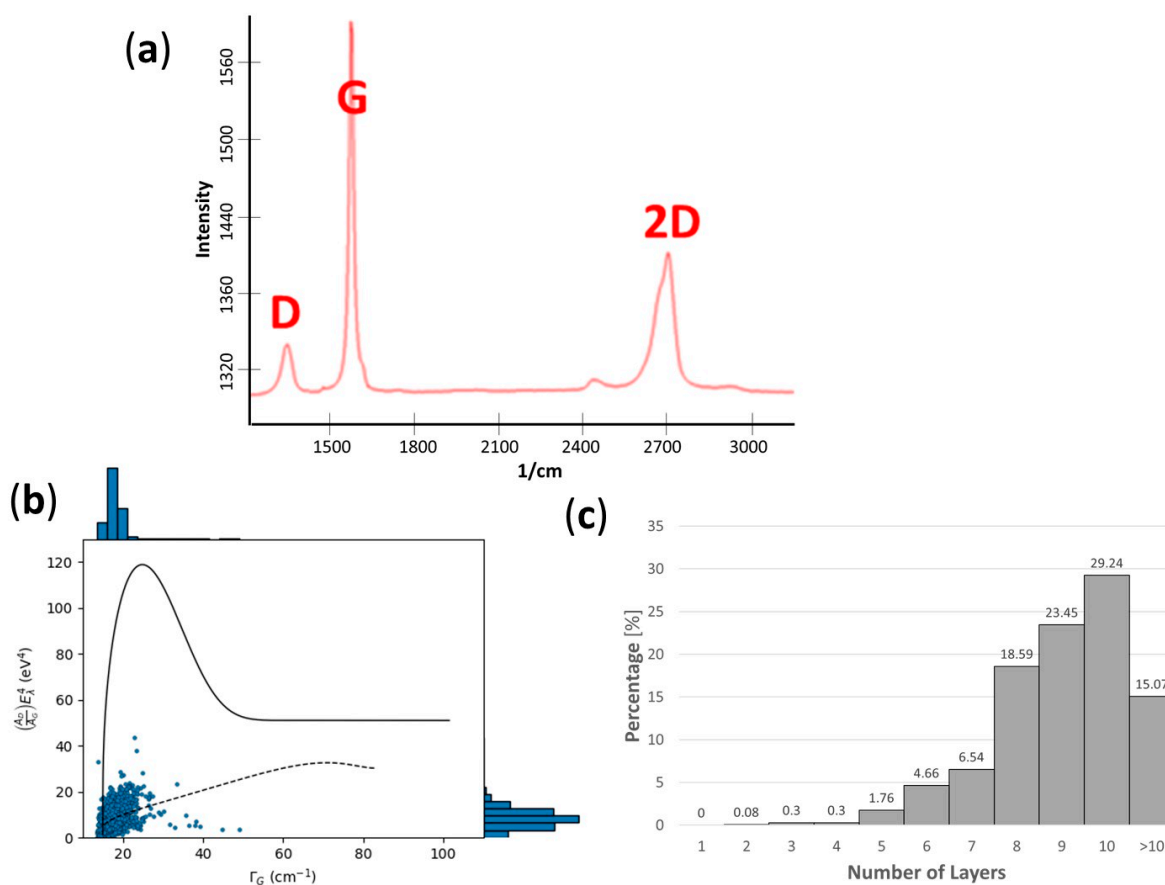


Figure 2. (a) Characteristic Raman spectrum. (b) Scatter plot with the frequency distributions of the G-band full-width at half-max (Γ_G) and the ratio between the integrated areas of the D and G bands (A_D/A_G) multiplied by the fourth power. (c) Layers Distribution.

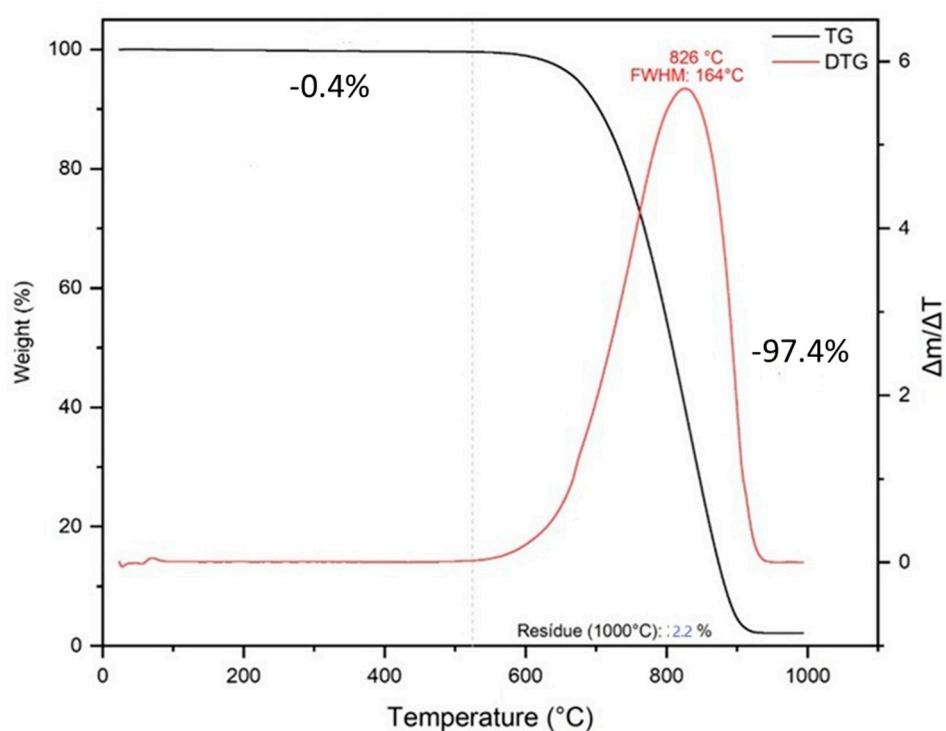


Figure 3. Thermogravimetric and derivative curves obtained under air gas flow of 100 mL/min and at a heating rate of 10 $^{\circ}\text{C}/\text{min}$.

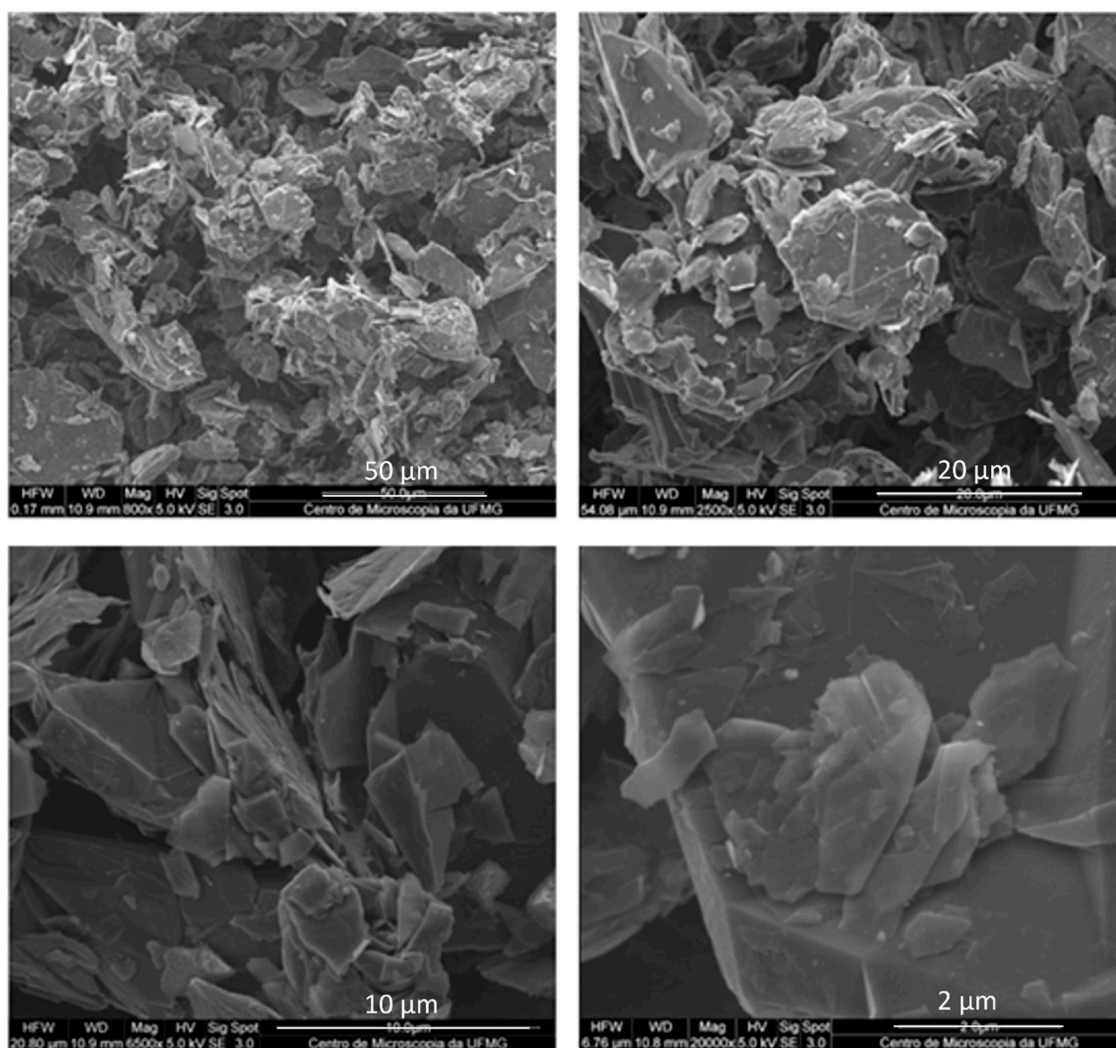


Figure 4. GNP scanning electron microscopy - SEM photos with crescent zooms.

2.2. Booster with Graphene

To ensure effective interaction between graphene and lubricants, a molecule featuring a highly reactive cyclic group and an oxygen functional group was used to functionalise the graphene powders (samples L66_1 and L66_2). This functionalization process was followed by treatment with an organic long-chain compound to enhance compatibility with the lubricant matrix. Both samples underwent advanced preparation methods tailored to optimize their performance in lubrication systems.

L66_1 was produced on an industrial scale using a high-energy mixing process, yielding a concentrated formulation with approximately 38% graphene nanoplatelets (GNP). L66_2, on the other hand, followed the same preparation method as L66_1 but incorporated an additional exfoliation step through purely shear mixing. This extra step was introduced to further reduce graphene aggregation, resulting in a more homogenous dispersion. The effectiveness of this modification was evidenced by a notable decrease in the viscosity of L66_2, see Figure 5.

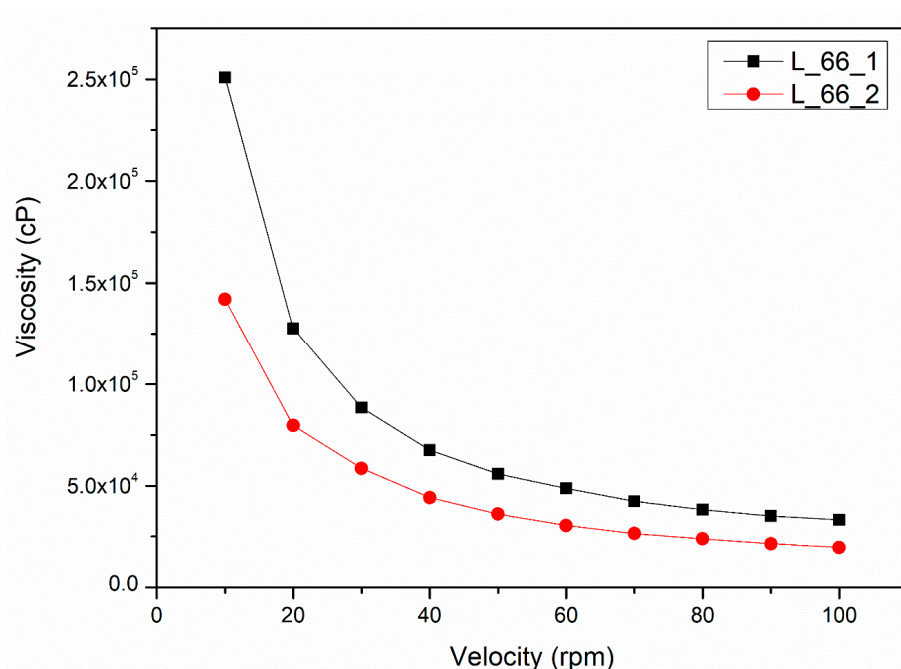


Figure 5. Viscosity of the additives L66_1 and L66_2.

The specific substances and techniques employed for graphene functionalization and mixing are proprietary and cannot be disclosed.

2.3. Reciprocating Friction Tests

For the tribological tests, the additives L66_1 and L66_2 were mixed with a fully formulated oil, SAE 0W-20 SN. To mix the GNP additives, the oil was heated to 40°C and the GNP mass required to achieve a 0.2 w/w% concentration was weighed on an analytical scale. The additive was then added to the warmed oil. The mixture was first stirred manually with a glass rod and then placed in an ultrasonic bath for 45 minutes. After this period, no sediment was observed. The mixture was stored, and photographs were taken as a function of time, as presented in Figure 6. Immediately after mixing (as new), and after 10 days, the dispersion remained visually stable. However, after 20 days, some sedimentation of the additive was observed at the bottom. The dispersion could easily be restored by gentle shaking and a brief ultrasonic bath treatment.

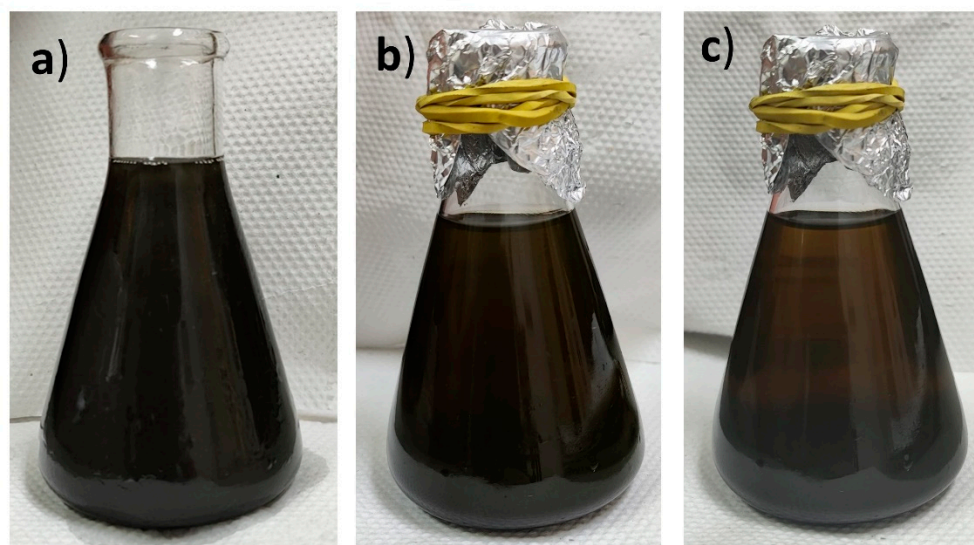


Figure 6. L66_1 on 0W20 (a) as new, (b) after 10 days (c) after 20 days,.

Tribological tests were conducted using an SRV tribometer (Optimol, Germany). This test involved the reciprocating sliding of a ball against the flat surface of a 24 mm diameter AISI H13 steel disc specimen. To ensure consistent roughness across all tests, the disc was polished, with the final polishing stage performed using a paste containing 1 μm diamond particles. After polishing, the surface roughness (S_a) was measured using a 3D laser interferometer. The ball was made of AISI 52100 steel, presenting a diameter of 10 mm. See Table 2.

Table 2. SRV sample parameters.

Sample	Diameter (mm)	Material	Hardness (Hv)	Young Modulus (GPa)	Poisson Ratio	Roughness S_a (μm)
Ball	10	AISI 52100	813 ± 6	210	0.3	0.042 ± 0.004
Disc	24	AISI H13	615	210	0.3	0.012 ± 0.002

Tribological tests were conducted in triplicate. Each repetition followed the procedure detailed in Table 3. Each repetition lasted 105 minutes, divided into steps of 15 minutes each. Five drops of oil were applied at each test start, covering the entire disc surface. After each test, residual oil was observed on the surface, indicating consistent lubrication throughout the test.

Table 3. Tribological test procedure.

Parameter	Unit					
Temperature	$^{\circ}\text{C}$	40		120		
Load	N	20	5	5	20	5
Max. Hertzian Pressure	GPa	1.2	0.5	0.5	1.1	0.5
Stroke	mm	5				
Frequency	Hz	5				
Duration	min/per step	15				

2.4. Vehicle Emission Tests

Vehicle tests were part of a larger test program comparing different lubricants and the GNP was added to a fully formulated 5W-20 oil. After the tests with SAE 5W-20 reference oil for the vehicle emission test, the engine was started and ran until the oil temperature reached the operation value, 90 $^{\circ}\text{C}$. The engine was stopped and 500 ml of oil was removed. From these, 250 ml was kept as a sample after the test and the other 250 ml, while still hot, was used to disperse the graphene additive. The mix was conducted only manually with the help of a “spoon”¹. Then the 250 ml plus additive was returned to the engine. The engine was completed with a volume of new oil considering the small amount of additive to ensure that the test sequence started with the same volume as with the reference oil. The engine was again restarted and run for a few minutes before being conditioned (“soaking period”) according to the test procedure standard. Brazil uses the so-called flex fuel and Brazilian standards (NBR) define fuel consumption in liters per 100 km, calculated from the balance of Carbon in the emissions to calculate the fuel mass converted to volume using the density of the test fuel.

The experimental emissions tests were performed with a large sport utility vehicle in an emissions laboratory following a combined cycle over a chassis dyno, according to NBR7024 [19],

¹ Such a simple mixing method was done to somehow mimic the expected application of the additive as a booster, on a common workshop.

composed of 55% in an urban cycle (FTP75) and 45% in a highway cycle. To better investigate the influence of the GNP additive, the urban, FTP75, cycle was divided in three phases: Ph1, Ph2 and Ph3. See Figure 7 and table 4. Ph3 has an identical vehicle speed profile as Ph1 but as the engine, and oil, are already hot, fuel consumption is significantly lower than on Ph1. Due to the temperature on the aftertreatment 3-way catalytic converter, almost all pollutant emissions occur on Ph1. See discussion on [13].

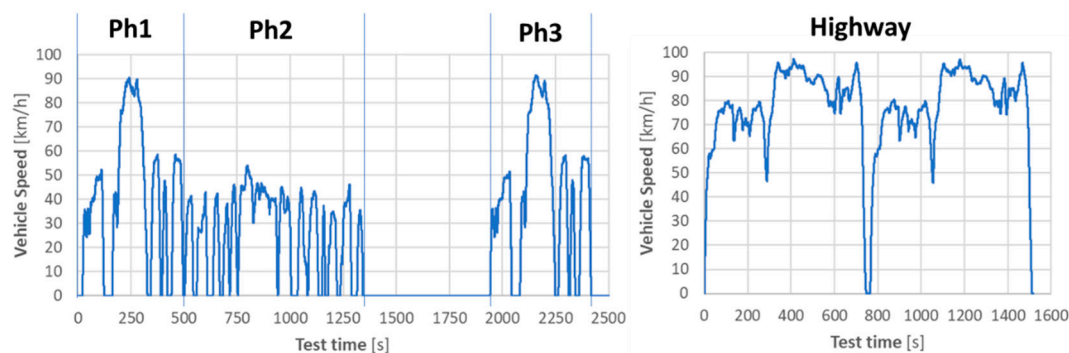


Figure 7. NBR7024 chassis emissions test. Ph1 to Ph3 are identical to the FTP75 emission test.

Table 4. Emission test cycle details.

	Units	Ph1 & 3	Ph2	Highway
Duration	s	505	864	765
Distance	km	5.78	6.21	16.45
Mean Velocity	km/h	41.20	25.88	77.73
Max. Velocity	km/h	91.2	55.2	96.56
Stops		6	13	None

The vehicle is equipped with a 4-cylinder, spark ignition, direct injection, turbocharged engine coupled to a 6-gear automatic transmission by a torque converter. At least two tests were performed with each lubricant version. The test uncertainties were compensated in terms of vehicle speed profile and battery voltage based on ECU data measurements by ETAS Inca. The test compensation factors were determined by 1-D numerical simulation with a vehicle mathematical model in a GT-Suite v.2024 from Gamma Technologies. The test compensation is detailed in [21].

3. Results

3.1. Reciprocating Friction Tests

The data was analyzed using the "all data" file generated by the SRV software. This file records CoF (Coefficient of Friction) data for one minute at intervals of 5 minutes, with measurements taken every 1.9×10^{-5} seconds during the recording minute. In this setup, each step consists of three such 5-minute intervals, totaling 15 minutes of testing under specific conditions (e.g., load or temperature). For each step, an average COF is calculated for the three individual measurements, and the overall CoF for the step is determined as the average of these three values. Figure 8 presents the CoF results for each step. Here, L66_1 and L66_2 refer to the dispersion of SAE 0W-20 with the respective additive variant.

Adding L66_1 and L66_2 decreased CoF compared to the reference oil, SAE 0W-20, under all test conditions. The CoF values for L66_1 and L66_2 were similar; L66_2 presented lower CoF than L66_1 in the first test steps, with the difference between the two additive variants reducing along the test. It can be speculated that along the test the GNP exfoliated in fewer layers and also created a

tribofilm in the surface. Such processes reduced the advantages of the more exfoliated and dispersed L66_2 in comparison to the 66_1 while in others, L66_1 shows a slight advantage. The largest difference between the L66 additives and the reference oil was observed in the test steps with 5N. The error bars in Figure 8 reflect the variation of COF during a single stroke, superimposed on the variations of COF throughout the strokes during the 15-minute evaluation period. Of these two causes, variations during the strokes may be significant, as presented in Figure 9, which reflects specific conditions at each contact point and the effect of the varying velocity during reciprocating motion. The lowest values of COF were obtained near mid-stroke, where higher velocities lead towards the hydrodynamic lubrication regime. Figure 7 also indicates a trend for larger error bars for the tests conducted with the lower 5 N, which impacts the measurement precision of the friction load.

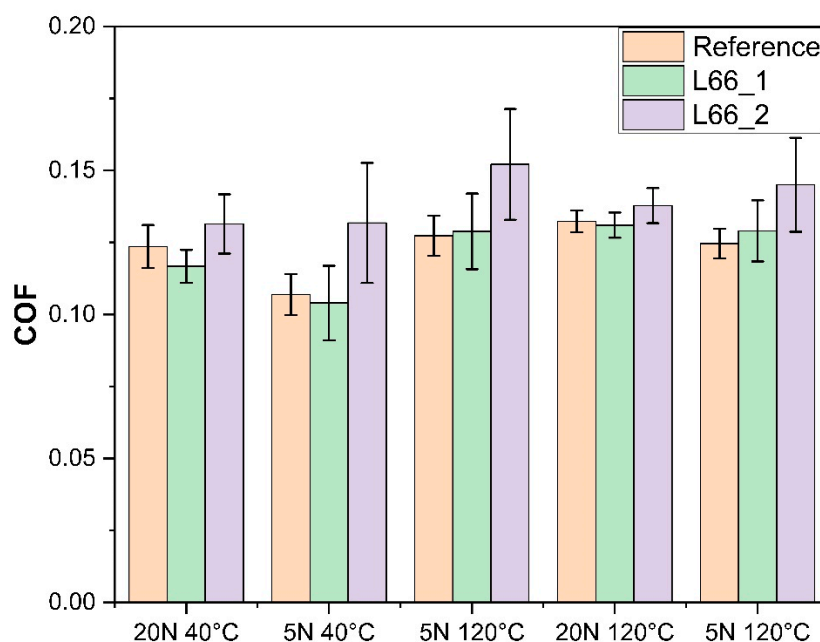


Figure 8. Cycle average CoF.

Another way to analyze the tribological results is in terms of friction losses. The energy dissipation due to the friction force is calculated through the force-displacement amplitude (F–D) hysteresis loops for each cycle during the test. Figure 9 shows one typical example of each lubricant variant and test step. Figure 10 shows the average results. As for the CoF, L66_2 presented a slight advantage compared to L66_1 in most of the test steps.

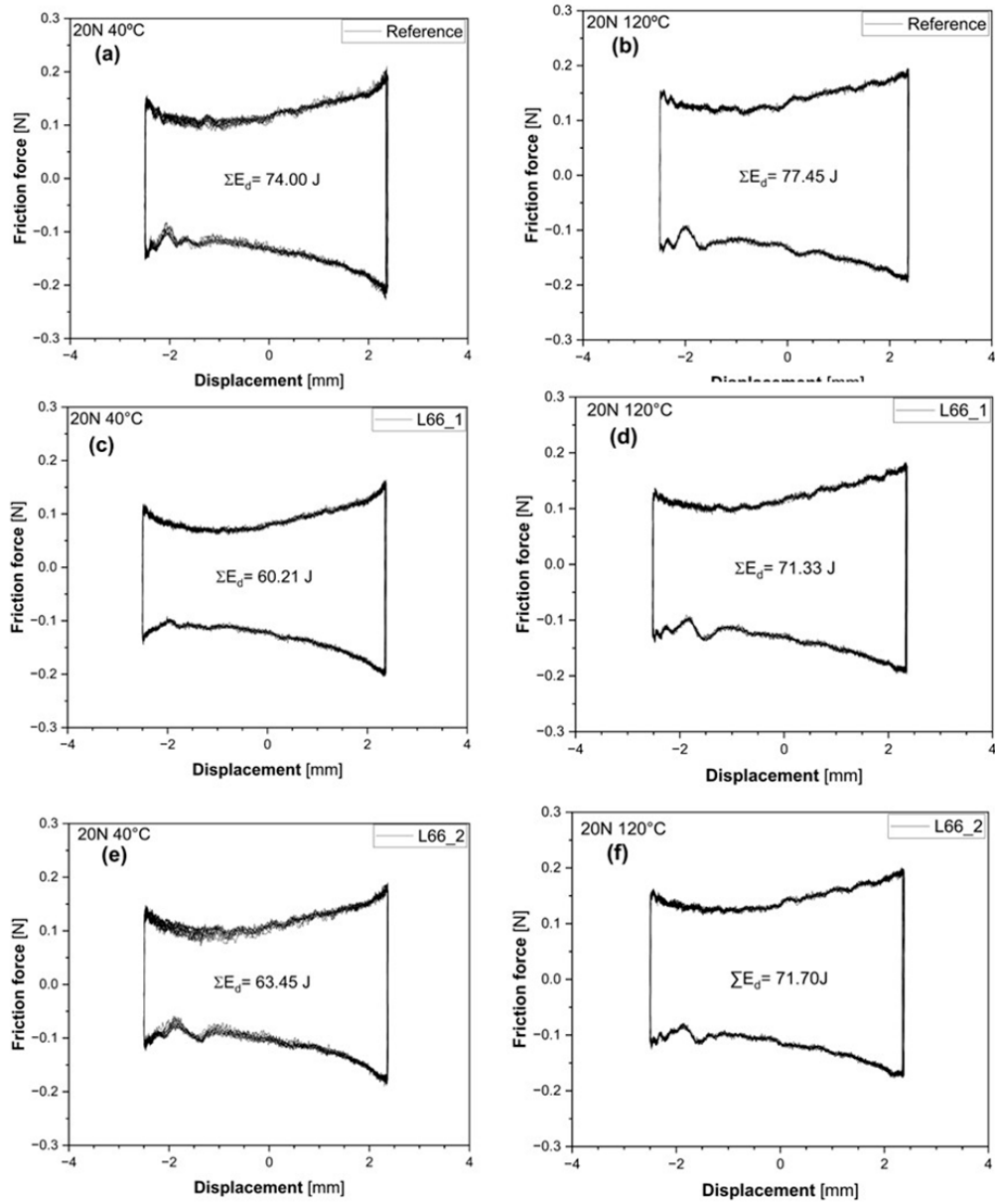


Figure 9. Friction force-displacement curves for the steps with 20N of applied load. (a–b), reference oil 0W-20m (c–d) with L66_1, (e–f) with L66_2.

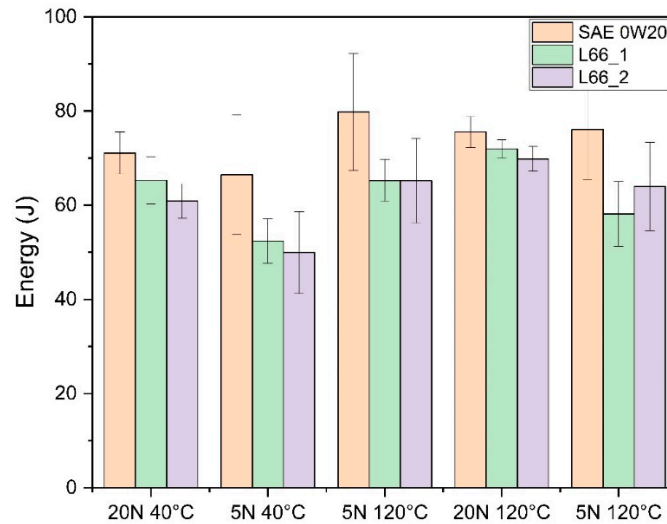


Figure 10. Dissipated Energy on the reciprocating tests.

3.2-. Fuel Consumption

As mentioned before, fuel consumption was measured by using the Carbon balance and converted to Liters per 100 km. To allow more detailed analysis, the FTP75 cycle was divided into three phases. Phase Ph1 and Ph3 have identical speed profiles, but Ph1 starts with the engine at room temperature, so oil viscosity is significantly higher than on Ph3. For this reason and to normal combustion issues, fuel consumption is also significantly higher on Ph1 than on Ph3. Figure 11 shows the delta fuel consumption (difference with respect to the consumption using the reference oil) in each of the three FTP75 phases, as well as the accumulated one, the one on Highway cycle and the NBR7024 that is composed of 55% of the FTP75 and 45% of the highway values. Compared with the 5W-20 reference oil, tests with additive presented a fuel saving of 2.6% on the FTP75, and 0.8% on the highway with the combined NBR2524 standard of 1.9% fuel saving. Figure 10 shows the range obtained with the minimum and average compensations described in [28]. The values in the plot refer to the ones with the average compensation.

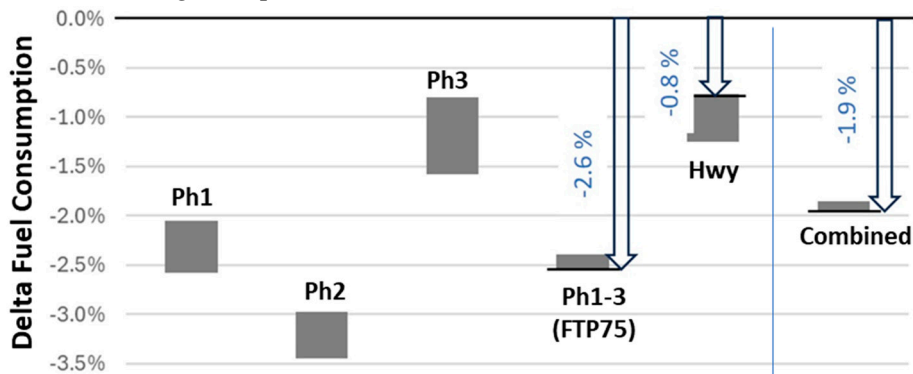


Figure 11. Delta fuel consumption with the L66_2, 0.1% GNP on the different test steps.

4. Discussion

Paying attention to Figure 11, it can be observed that, as expected, fuel-saving reductions with the GNP additive were more significant on the Ph1 and Ph2 phases, where friction losses have more impact on fuel consumption. Internal combustion engines present several lubricated systems, which vary in terms of the predominant lubrication regime. In part of the systems, such as in cam-follower, the boundary lubrication may prevail, while in journal bearings hydrodynamic lubrication is expected to be the most important. Thus, the decrease in fuel consumption with the use of the GNP

additives can be due to both boundary and hydrodynamic effects. Besides, graphene additives have shown the potential of increasing the lubricant conductivity. On the conducted tests, the oil with GNP additive showed a slighter quicker temperature drop during the vehicle stop interval between the cold and hot phases. See Figure 12. Such behavior suggests that the addition of graphene increased the oil thermal conductivity as seen by other authors. Alqahtani [23] obtained a 20% increase in thermal conductivity on a SAE 5W-30 with a concentration of 0.09 wt% of graphene. A similar increase of thermal conductivity was seen on [24,25]. In the vehicle test described in this work, the oil with GNP started the hot phase approximately 2°C cooler. The impact on viscosity is negligible, but such an increase in thermal conductivity could be beneficial in terms of wear and on applications such Electrical Vehicles [26] and rolling bearings [24,27].

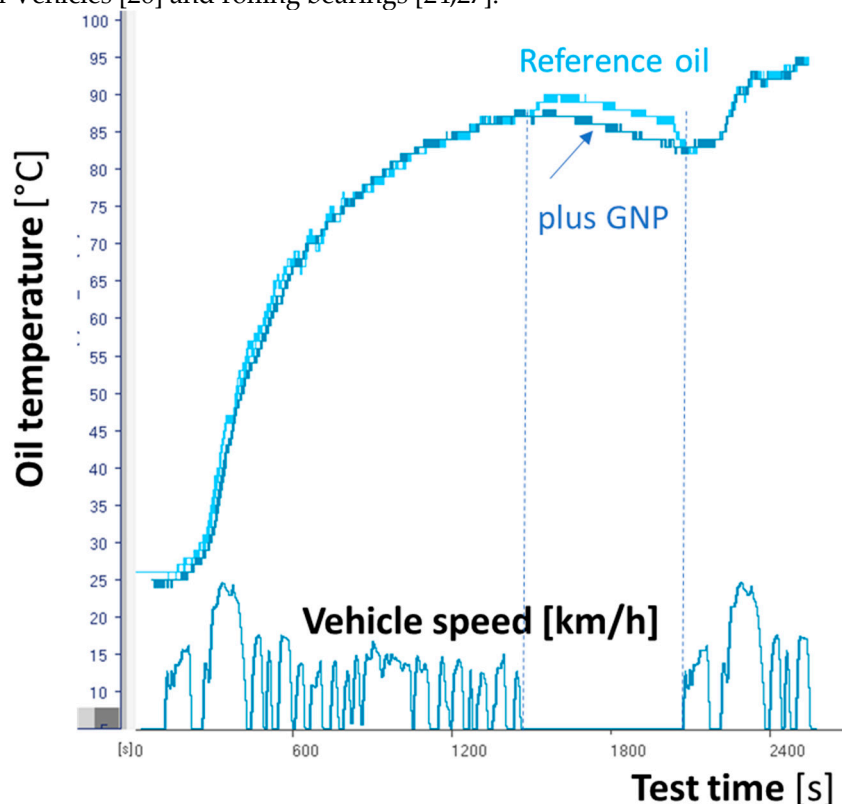


Figure 12. Oil temperature along the test.

5. Conclusions

The use of Graphene nanoplatelets, with an average of 9 layers, after functionalization to work as a lubricant additive, reduced both CoF and friction losses on a reciprocating test. Specifically at the more severe test condition, of 40N and 120 °C, the L66_2 additive reduced the CoF and the Energy losses in 5% and 8%, respectively, in comparison with the reference oil, a fully formulated SAE 0W-20.

On vehicle emission tests, adding 0.1% w/w of GNP on a fully formulated 5W-20 SAE oil reduced fuel consumption by 2.6% in the FTP-75 cycle and 0.8% in the Highway, resulting in 1.9% in the combined cycle.

The conducted work showed promising fuel savings on SI engines under vehicle emission tests. This work is part of a larger project where durability and additive degradation are key factors. Additive selection is especially important for Diesel engines, where MoDTC is not used because it causes clogging in the Diesel Particulate Filter (DPF). As with other friction modifier additives, the benefits of using GNP are expected to be higher on oils with ultra-low viscosity.

Author Contributions: “Conceptualization, E.T., F.R.; investigation, W.C., P.G., D.F., R.S., F.R.; resources, W.C., P.G., S.R., J.C., R.S., F.R.; writing—original draft preparation, E.T., F.R.; writing—review and editing, all authors. All authors have read and agreed to the published version of the manuscript.”

Funding: Part of this work was funded by the “Fundação da Universidade Federal do Paraná” with the project 27192.24, ROTA2030

Conflicts of Interest: The authors declare no conflicts of interest

References

1. Tormos, B.; Pla, B.; Bastidas, S.; Ramírez, L.; Pérez, T.; Fuel economy optimization from the interaction between engine oil and driving conditions, *Tribology International*, Volume 138, 2019, Pages 263-270, ISSN 0301-679X, <https://doi.org/10.1016/j.triboint.2019.05.042>
2. Taylor, R.; Morgan, N.; Mainwaring, R.; Davenport T.; How much mixed/boundary friction is there in an engine — and where is it? *Proceedings of the Institution of Mechanical Engineers, Part J: Journal of Engineering Tribology*. 2020;234(10):1563-1579. doi:10.1177/1350650119875316
3. Kennedy, M.; Hoppe, S.; Esser, J. Weniger Reibleistung Durch Neue Kolbenringbeschichtung. *MTZ - Motortechnische Zeitschrift* 2014, 75, 48–51, doi:10.1007/s35146-014-0316-6.
4. Schommers, J.; Scheib, H.; Hartweg, M.; Bosler, A. Reibungsminimierung Bei Verbrennungsmotoren. *MTZ - Motortechnische Zeitschrift* 2013, 74, 566–573, doi:10.1007/s35146-013-0170-y.
5. Tamura, K.; Kasai, M.; Nakamura, Y.; Enomoto, T. Impact of Boundary Lubrication Performance of Engine Oils on Friction at Piston Ring-Cylinder Liner Interface. *SAE Int J Fuels Lubr* 2014, 7, 875–881, doi:10.4271/2014-01-2787.
6. Tamura, K.; Kasai, M.; Nakamura, Y.; Enomoto, T. Influence of Shear-Thinning of Polymer-Containing Engine Oils on Friction at the Piston Ring-Cylinder Liner Interface. In *Proceedings of the SAE Technical Papers*; SAE International, 2013; Vol. 11.
7. Michlberger, A.; Morgan, P.; Delbridge, E.E.; Gieselman, M.D.; Kocsis, M. Engine Oil Fuel Economy Testing - A Tale of Two Tests. *SAE Int J Fuels Lubr* 2017, 10, 478–486.
8. Holmberg, K., Andersson, P. and Erdemir, A., Global Energy Consumption Due to Friction in Passenger Cars, *Tribology International*, vol. 47, pp. 221–34, March 2012. DOI: 10.1016/j.triboint.2011.11.022.
9. Spikes H (2015) Friction modifier additives. *Tribol Lett* 60:1–26
10. Y.Y. Wu, W.C. Tsui, T.C. Liu. Experimental analysis of tribological properties of lubricating oils with nanoparticle additives. *Wear* 262 (2007) 819–825
11. M. Gulzar . H. H. Masjuki . M. A. Kalam . M. Varman . N. W. M. Zulkifli . R. A. Mufti. Rehan Zahid Tribological performance of nanoparticles as lubricating oil additives. *J Nanopart Res* (2016) 18:223 DOI 10.1007/s11051-016-3537-4
12. Shahnazar, S., Bagheri, S., Hamid, S.. Enhancing lubricant properties by nanoparticle additives. *International journal of hydrogen energy* 41 (2016) 3153 e3 170.
13. Tomanik, E.; Christinelli, W.; Souza, R.M.; Oliveira, V.L.; Ferreira, F.; Zhmud, B. Review of Graphene-Based Materials for Tribological Engineering Applications. *Eng* 2023, 4, 2764-2811. <https://doi.org/10.3390/eng4040157>
14. Nyholm, N.; Espallargas, N. Functionalized carbon nanostructures as lubricant additives—A review. *Carbon* 2023, 201, 1200–1228

15. Gao, Jingde, et al. "Dialkyl Dithiophosphate-Functionalized Ti₃C₂T_x MXene Nanosheets as Effective Lubricant Additives for Antiwear and Friction Reduction." *ACS Applied Nano Materials* 4.10 (2021): 11080-11087.
16. Guido Boidi, João C. F. de Queiróz, Francisco J. Profito, and Andreas Rosenkranz Ti₃C₂T_x MXene Nanosheets as Lubricant Additives to Lower Friction under High Loads, Sliding Ratios, and Elevated Temperatures. *ACS Applied Nano Materials* 2023 6 (1), 729-737. DOI: 10.1021/acsnm.2c05033
17. Singh, A., Dwivedi, R. and Suhane, A.. In the Context of Nano Lubrication, Do Nanoparticles Exhibit Favourable Impacts on All Tribo Surfaces? A Review. ISSN 2070-2051, *Protection of Metals and Physical Chemistry of Surfaces*, 2022, Vol. 58, No. 2, pp. 325–338. © Pleiades Publishing, Ltd., 2022. DOI: 10.1134/S2070205122020174
18. Silva, D.L.; Campos, J.L.E.; Fernandes, T.F.; Rocha, J.N.; Machado, L.R.; Soares, E.M.; Miquita, D.R.; Miranda, H.; Rabelo, C.; Neto, O.P.V.; et al. Raman spectroscopy analysis of number of layers in mass-produced graphene flakes. *Carbon* 2020, 161, 181–189.
19. NBR7024, ASSOCIAÇÃO BRASILEIRA DE NORMAS TÉCNICAS (ABNT). NBR7024: Veículos rodoviários automotores leves – Medição do consumo de combustível – Método de ensaio. Rio de Janeiro, 2010, 13p.
20. Tomanik, E., Miedviedieva, N., Tomanik, V., Miedviediev, B., Use of digital twins to analyze and predict CO₂ and emissions on Hybrid vehicles. International Scientific Conference INTELLIGENT TRANSPORT SYSTEMS: Ecology, Safety, Quality, Comfort. Kiev, Ukraine, November 26-27, 2024.
21. Rovai, F., Tomanik, E. "Lubricant viscosity impact in fuel economy: experimental un-certainties compensation". *Lubricants* 2025, to be published
22. Rustamov, I., Xiang, L., Xia, Y., Peng W., Tribological and mechanical endowments of polyoxymethylene by liquid-phase exfoliated graphene nanofiller. *Polymer International*, 2024, <https://doi.org/10.1002/pi.6712>.
23. Alqahtani, B.; Hoziefa, W.; Abdel Moneam, H.M.; Hamoud, M.; Salunkhe, S.; Elshalakany, A.B.; Abdel-Mottaleb, M.; Davim, J.P. Tribological Performance and Rheological Properties of Engine Oil with Graphene Nano-Additives. *Lubricants* 2022, 10, 137. <https://doi.org/10.3390/lubricants10070137>
24. Ota, J.; Hait, S.; Sastry M.; Ramakumar, S. Graphene dispersion in hydrocarbon medium and its application in lubricant technology. *RSC Adv.*, 2015, 5, 53326. DOI: 10.1039/c5ra06596h
25. Contreras E., G. Oliveira, E. Bandarra. Experimental analysis of the thermohydraulic performance of graphene and silver nanofluids in automotive cooling systems, *International Journal of Heat and Mass Transfer*, V. 132, 2019, pp.375-387, ISSN 0017-9310, <https://doi.org/10.1016/j.ijheatmasstransfer.2018.12.014>.
26. Canter N., *Tribology and Lubrication for E-Mobility: Findings from the Inaugural STLE Conference on Electric Vehicles*, 2022
27. Nassef, M.; Soliman, M.; Nassef, B.; Daha, M.; Nassef, G. Impact of Graphene Nano-Additives to Lithium Grease on the Dynamic and Tribological Behavior of Rolling Bearings. *Lubricants* 2022, 10, 29. <https://doi.org/10.3390/lubricants10020029>

Disclaimer/Publisher's Note: The statements, opinions and data contained in all publications are solely those of the individual author(s) and contributor(s) and not of MDPI and/or the editor(s). MDPI and/or the editor(s) disclaim responsibility for any injury to people or property resulting from any ideas, methods, instructions or products referred to in the content.